CHEMISTRY
A European Journal

A Journal of
ChemPubSoc Europe

Accepted Article

Title: Color-Tunable Light-up Bioorthogonal Probes for in-vivo Two-Photon Fluorescence Imaging

Authors: Yandong Dou, Yajun Wang, Yukun Duan, Bin Liu, Qinglian Hu, Wei Shen, Hongyan Sun, and Qing Zhu

To be cited as: *Chem. Eur. J.* 10.1002/chem.201905183

Link to VoR: http://dx.doi.org/10.1002/chem.201905183

Supported by
ACES

WILEY-VCH

10.1002/chem.201905183

WILEY-VCH

FULL PAPER

Color-Tunable Light-up Bioorthogonal Probes for in-vivo Two-Photon Fluorescence Imaging

Yandong Dou,[+][a] Yajun Wang,[+][a] Yukun Duan,[b] Bin Liu,*[b] Qinglian Hu,[a] Wei Shen, *[c] Hongyan Sun*[d] and Qing Zhu*[a]

Abstract: Light-up bioorthogonal probes have attracted increasing attention recently due to their capability of direct imaging of di-verse biomolecules in living cells without washing steps. The development of bioorthogonal probes with excellent fluorescent properties suitable for in-vivo imaging, such as long excitation/emission wavelength, high fluorescence turn-on ratio, and deep penetration has been rarely reported. Herein, we design and synthesize a series of azide-based light-up bioorthogonal probes with tunable colors based on a weak fluorescent scaffold of 8-aminoquinoline (**AQ**). The azido quinoline derivatives are able to induce large fluorescence enhancement (up to 1352-fold) after click reaction with alkynes. In addition, the probes could be engineered to display excellent two-photon property (δ = 542 GM at 780 nm) after further introducing different styryl groups into the **AQ** scaffold. Subsequent detailed bioimaging experiments demonstrate that these probes are versatile, which have been successfully used for live cell/zebrafish imaging without washing steps. Further in vivo two-photon imaging experiments demonstrated that these newly developed light-up biorthogonal probe outperformed the conventional fluorophores, e.g. high signal-to-noise ratio and deep tissue penetration. The design strategy reported in this study represents a useful approach to realize a diversity of high-performance biorthogonal light up probes for in vivo studying.

Introduction

Fluorescence imaging has been a powerful technique for investigating biological molecules in living organisms with superb spatiotemporal resolution.[1-2] Traditional fluorophores for fluorescent imaging usually display strong back-ground fluorescence, which requires extensive washing steps.[3] To address this issue, a class of light-up bioorthogonal probes has emerged, which attracts intense attention from scientific community.[4-6] These probes are usually consisted of two parts, a fluorophore and a bioorthogonal group which also acts as a quencher. Upon reacting with their bioorthogonal counterparts, large fluorescence turn-on is induced which allows for real-time imaging without washing steps. So far, bioorthogonal labeling has been employed for in vitro imaging of various molecules, e.g. small molecule drugs, natural products and proteins.[7-9]

During the past few years, considerable efforts have been made on extracellular or intracellular turn-on bioimaging with azide-/tetrazine fluorogenic probes in living cells.[10-12] These probes could undergo bioorthogonal reaction via copper catalyzed (CuAAc) or "Diels–Alder" cycloaddition, respectively.[13-16] So far, azide-based light-up bioorthogonal probes have attracted considerable attention due to their small size and high quenching efficiency.[17] For example, Wong[18] designed an azido-BODIPY based probe AzBOCEt (Az10), which can induce up to 52-fold fluorescence enhancement after click reaction (Fig. 1a). Based on the principle of photo-induced electron transfer (PeT), Bertozzi elegantly designed a panel of fluorogenic azide probes that can be activated via click chemistry (Fig. 1a).[19] Besides high fluorescence turn-on efficiency, attempts have also been made to develop fluorescent derivatives covering a wide range of emission wavelengths based on monochromophoric design.[20] Despite many successful examples for in-vitro studying, in-vivo experiments are less explored as they require long wavelength excitation and large turn-on ratios to differentiate the signal from auto-fluorescence of bio-substrates.

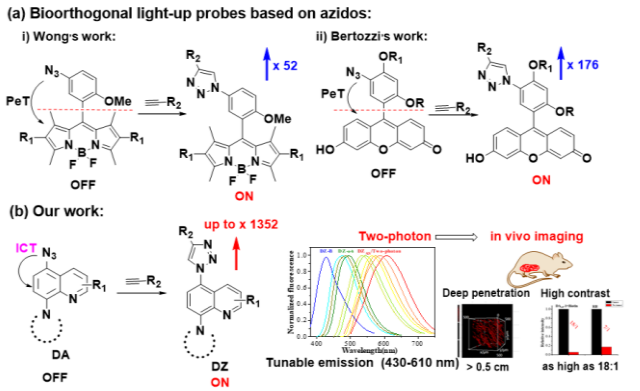

Fig. 1. (a) Classical light-up fluorophores based on PeT mechanism; (b) Our strategy for designing light-up bioorthogonal probes based on ICT mechanism.

Herein, we report a new class of color-tunable two-photon light-up bioorthogonal probes based on a fluorescent scaffold of 8-aminoquinoline (AQ) (Fig. 1b). Specifically, we achieved site-specific introduction of azido group at the C-5 position of AQ via C-H/I activation. The azido-AQ derivatives showed low

[a] Y. Dou, Dr. Y. Wang, Dr. Q. Hu, Prof. Q. Zhu
College of Biotechnology and Bioengineering, Zhejiang University of Technology, Hangzhou 310014, China E-mail: zhuq@zjut.edu.cn
[+] These authors contributed equally to this work
[b] Y. Duan, Prof. Dr B. Liu
Department of Chemical and Biomolecular Engineering, National University of Singapore, 4 Science Drive 4 117585, Singapore
E-mail: cheliub@nus.edu.sg
[c] W. Shen
Department of General Surgery, Jinhua Municipal Central Hospital, Jinhua 321000, China，E-mail: zhuqshenw@hotmail.com
[d] Prof. H. Sun
Department of Chemistry, City University of Hong Kong, 83 Tat Chee Avenue, Kowloon, Hong Kong, China
E-mail: hongysun@cityu.edu.hk

Supporting information for this article is given via a link at the end of the document.((Please delete this text if not appropriate))

10.1002/chem.201905183

fluorescence background due to intramolecular charge transfer (ICT) effect, whereas they could generate high fluorescence after click reaction (~700-fold turn-on). The emission wavelength of the clicked triazole fluorophores can be fine-tuned from 430 to 610 nm. Remarkably, higher quantum yields, larger fluorescence enhancement (up to 1352-fold) and longer emission wavelength (610 nm) could be achieved by introducing an aziridine ring and a styryl group to AQ. The values of these probes have been further demonstrated in two-photon imaging of living cells, and zebrafishes without washing steps. The in vivo imaging of mice demonstrated that these newly developed light-up biorthogonal probe displayed much higher signal-to-noise ratio and deeper penetration than the conventional fluorophores.

Results and Discussion

8-Aminoquinoline was chosen in our study due to its simple and easily-modifiable structure. The introduction of azide group could diminish the fluorescence background due to ICT quenching effect.[21-22] On the other hand, trans-formation of the azide to triazole group will not only sup-press ICT effect, but also enlarge the conjugation system of the fluorophore to yield tunable emission.[23] We envision that azido substituted 8-aminoquine derivatives will serve as an excellent building block to construct a new class of highly fluorogenic biorthogonal probes.

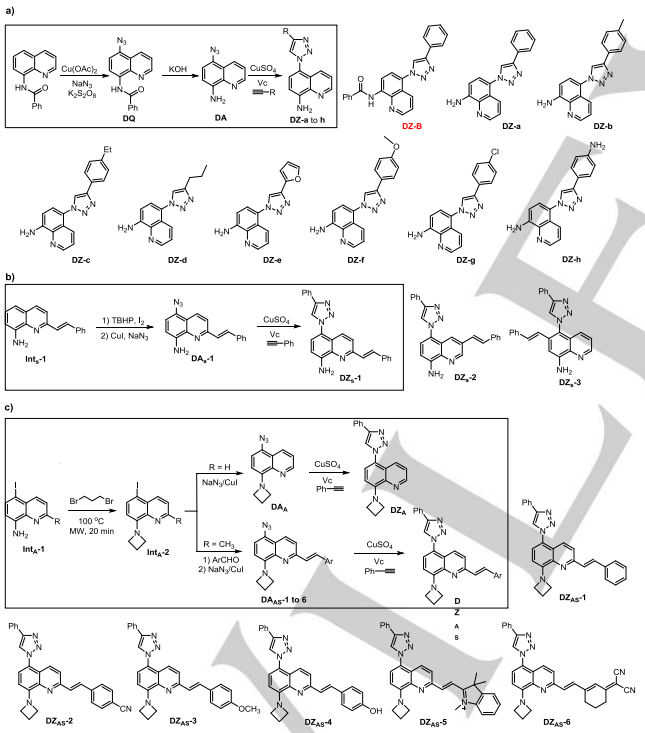

Scheme 1. The general synthetic pathway of the bioorthogonal probes and the structures after click reaction. a) Synthetic pathway of **DA** bioorthogonal probes and its triazole derivatives (**DZ-a-h**); b) Synthetic pathway of the second generation of probes with long emission wavelength: styryl substituted 5-azido-8-aminesquinolines (**DA$_S$**) and their triazole derivatives (**DZ$_S$-1-3**); c) Synthetic pathway for two-photon light-up probes DA$_{AS}$ by introducing an aziridine ring and a styryl group to AQ.

To verify our design, 5-azido-8-aminoquinoline (DA) was firstly synthesized via C-H azidation of AQ under mild condition (Scheme 1a).[24-25] Briefly, AQ was firstly treated with benzoyl chloride in the presence of triethyl amine to afford N-benzoyl 8-aminoquinoline. Then azidation was carried out utilizing $Cu(OAc)_2$ as catalyst and NaN_3 as the azido source to give **DQ**, which was hydrolyzed in potassium hydroxide to offer **DA** in 75% yield. Subsequently, the click reactions between **DA** and different alkynes, including aromatic and aliphatic substituted alkynes, were carried out. The corresponding triazoles **DZ-a~h** were obtained in more than 90% yields.

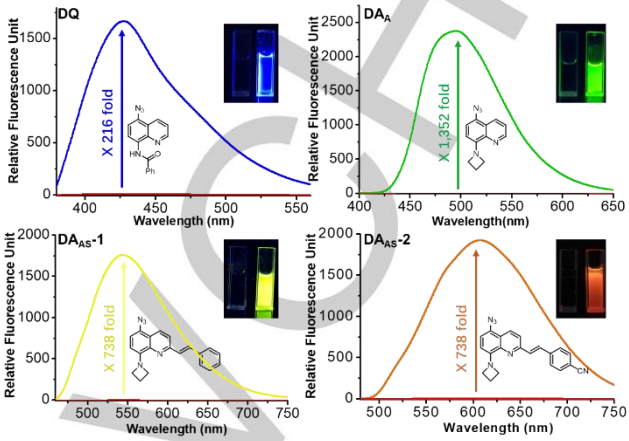

Fig. 2. Fluorescence enhancements of DQ, DA$_A$, DA$_{AS}$-1 and DA$_{AS}$-2 after copper-catalyzed click reactions. Reaction condition: CuSO4·5H2O (20 μM) and sodium ascorbate (40 μM) were added to a mixture of ethynylbenzene (20 μM) and azido-fluorophore (10 μM), and fluorescence intensity was monitored after 30 min at 25 °C in PBS solution (20 mM, pH 7.4, 10% DMSO).

With these compounds in hand, we firstly investigated the fluorescent properties of **DA** and its triazole derivatives **DZ-a~DZ-h**. Although **DA** has an absorption at 350 nm, it showed weak fluorescence due to the quenching effect of the electron-rich azide group via ICT mechanism (Fig. S1–S2).[26] The triazole derivatives displayed absorptions at around 365 nm with strong fluorescence in 480-524 nm range (Fig. S2–S3) showing the turn-on ratios ranging from 630 to 730-fold in H_2O after click reaction (Table S1). However, when the triazole is bearing an electron withdrawing group (**DZ-g**), its fluorescent intensity could increase along with a distinct blue shift of the emission. Interestingly, the emission of **DZ-h** displays red-shift at 524 nm in DMSO and 500 nm in pure water. This phenomenon could be attributed to that the electron-donating group improves the energy of HOMO and LOMO level, while the HOMO is improved more significantly, resulting in the red-shift emission (Figure S6). Moreover, no significant influence of the substituent at the triazole on the excitation wavelengths was observed. These results demonstrate that our first generation of light-up bio-orthogonal probe is capable of fluorescence turn on after cycloaddition reaction.

To red-shift the absorption and emission of AQ based probes, we introduced styrene at C-2, C-3, and C-6 of AQ to systematically study the structure-property relationship. Firstly, 2-styrylquinolin-8-amine was iodinated, followed by the substitution with NaN_3 in the presence of CuI, to afford **DA$_S$-1** (Scheme 1b, Scheme S2). Following a similar route, C-3/-6 vinyl substituted **DA$_S$-2** and **DA$_S$-3** were successfully obtained in good yields (Scheme 1a, Scheme S2~S4). The click reaction with ethynylbenzene gave the corresponding triazoles **DZ$_S$-1~3**. To our delight that the introduction of vinyl group could red-shift the absorption to around 380 nm and extend the emission wavelength effectively from 486 nm to 540 nm (Figure S7~S8). It is noteworthy that, while **DZ$_S$-1~3** exhibit similar emission wavelength around 540 nm, the C-2 substitution gave the highest fluorescence quantum yield (Φ= 0.374) and turn-on ratio (238-fold) (Table S2). Therefore, C-2 substitution was selected for subsequent studies.

10.1002/chem.201905183

As the intramolecular hydrogen bond between the amino group (C-8 position) and nitro atom (C-1 position) of 8-aminoquinoline is highly prone to decrease the fluorescent signal because of the excited-state proton transfer (ESPT) effect.[27] To reduce the impact of environmental factor and further enhance the fluorescence quantum yield of the bio-orthogonal product,28 we attempted to replace the amino group at C-8 position of the quinoline with a dialkylated amino group (Scheme 1c, Scheme S5), and to our delight, a four-membered azetidine displays the higher quantum yield and its emission wavelength red-shits 10 nm (Figure S9). Furthermore, various vinyl containing building blocks, such as styryl groups with electron withdrawing (**DZ_{AS}-2**) and donating groups (**DZ_{AS}-3, 4**), 2-vinyl indole and 2-(3-vinylcyclohex-2-en-1-ylidene) malononitrile are introduced to AQ scaffold to further red-shift the emission wavelength. To obtain 2-styryl-8-(1-azetidinyl)-quinolines (**DA_{AS}**), 5-iodo-2-methylquinolin-8-amine (**IntA-1**) and 1,3-dibromopropane were incubated together in a microwave oven to yield the four-membered azetidine substituted qunioline **IntA-2**. Next, **IntA-2** was condensed with different aldehydes to give 2-styryl substituted compounds **IntA-3**, which were subjected to Cu(I)-catalyzed C-I azidation to afford various molecules **DA_A** and **DA_{AS}-1~6** (Scheme 1c, Scheme S6). Subsequently, their triazoles **DZ_A** and **DZ_{AS}-1~6** derivatives could be obtained readily via click reaction with ethynylbenzene. To our delight, the emission wave-length is red-shifted to 610 nm when 4-methylbenzonitrile was conjugated with quinoline (**DZ_{AS}-2**) (Table S3).

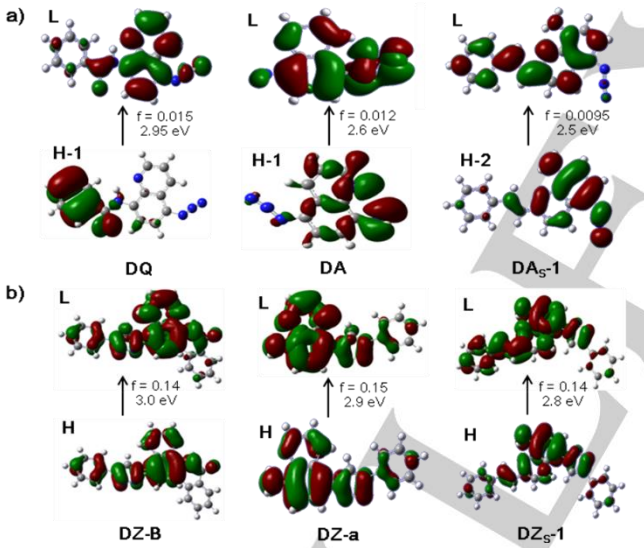

Fig. 3. Molecular orbital distribution vertical transition energy and oscillator strength values (f) .a) **DQ, DA, DA_S-1** from left to right by TD-DFT calculation (CAM-B3LYP/6-31G*) of the corresponding first excited-state optimized structures. H and L stand for HOMO and LUMO, respectively. b) after click reaction obtained by TD-DFT calculation (CAM-B3LYP/6-31G*) of the corresponding first excited-state optimized structures. H and L stand for HOMO and LUMO, respectively.

Next, we studied the fluorescence turn-on response of the probes before and after click reactions. As shown in Table S1-S3, all of these compounds display excellent turn-on ratios. Specifically, **DQ**, **DA_A**, **DA_{AS}-1, DA_{AS}-2** were treated with ethynylbenzene, $CuSO_4{\cdot}5H_2O$ and sodium ascorbate for 30 min to generate the corresponding fluorophores of **DZ-B**, **DZ_A**, **DZ_{AS}-1**, **DZ_{AS}-2**. Their emission wavelengths cover from blue to red (430 to 610 nm), and the fluorescence turn-on ratios were determined as 216 (**DQ** to **DZ-B**), 1352 (**DA_A** to **DZ_A**), 738 (**DA_{AS}-1** to **$DZ_{AS\text{-}1}$**), and 352 (**DA_{AS}-2** to **$DZ_{AS\text{-}1}$-2**) folds, respectively (Fig. 2). Therefore, those probes constructed from 8-aminequinoline could be further easily modified to offer a series of new fluorophores covering different colors with excellent fluorescence turn-on properties.

It was also found that the Cu-catalyzed alkyne-azide cycloaddition could achieve 85% conversion within 30 min (Fig. S10, S11), which was fast enough for most applications.[29] A fast reaction kinetic (k_2) of **DA_A** was obtained as 11.5 M^{-1} s^{-1} in PBS by treatment with ethynylbenzene (Fig. S12). These results indicate that our bioorthogonal probes can generate light-up fluorescent signal effectively for biomedical application.

To understand the low background signal and the fluorescence turn-on, we further carried out time-dependent density functional theory (TD-DFT) calculations (CAM-B3LYP/6-31G*).[30] As shown in Fig. 3, the main orbitals contributing to the S_0-S_1 transition of azide-based probes is an π→π* type transition. Based on the lowest first singlet excited state of azide-based probes, the nonbonding orbitals largely contribute to the π→π* transition. Meanwhile, the optically inactive π→π* transition at the lowest lying state disappears after click reaction with extended aromatic systems, but the n→π* transition becomes the most important transition between the S_0 and S_1 states in all triazole-structures (Table S4, Table S5).[31] Moreover, f values for the S_0-S_1 transition in triazole-structures (from 0.14 to 0.15) are significantly higher than that of the S_0−S_1 transition in azide structures (from 0.0095 to 0.015). The high f values of triazole-structures indicate that the excited fluorophores could lose radiative energy after click reaction. Taken together, computational calculation demonstrates that azide moiety in the molecule causes the optically inactive π→π* transition and low f value of the major S_0−S_1 transition, and thus result in quenching the fluorescence of the chromophores.

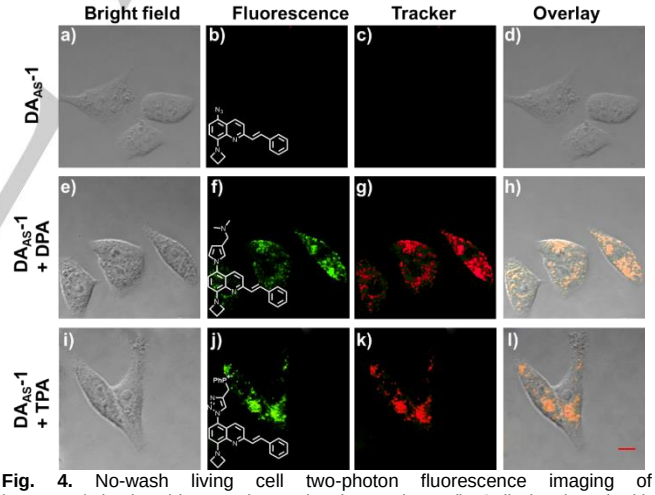

Fig. 4. No-wash living cell two-photon fluorescence imaging of lysosome/mitochondria-targeting molecules. a, b, c, d): Cells incubated with **DA_{AS}-1** (5 μM); e, f, g, h): Cells incubated with **DA_{AS}-1** (5 μM) THPTA (10 μM), $CuSO_4{\cdot}5H_2O$ (10.0 μM), sodium ascorbate (20 μM) *N, N*-dimethylprop-2-yn-1-amine (**DPA**)(10 μM) and DND-99 (100 nM) as the lysosomes tracker; I, j, k, l) **DA_{AS}-1** (5.0 μM) THPTA(10 μM), $CuSO_4{\cdot}5H_2O$ (10 μM), sodium ascorbate (20 μM), triphenyl phosphine-alkyene(**TPA**) (10 μM) and Mito-Red-FM (500 nM) as the mitochondria tracker; b ,c, f, j) Ex = 780 nm, Em = 520 nm-580 nm; g) Ex = 1040 nm, Em = 560-600 nm; k) Ex = 1040 nm, Em = 620-650 nm); a, e, i) Bright light; d, h, l) Overlay. Scale bar: 20 μm.

Compared to one-photon imaging, two-photon (TP) imaging possesses distinct advantages, including increased penetration depth and reduced specimen photodamage due to its longer excitation wavelength. Specifically, the two-photon increased penetration depth and reduced specimen photodamage due to its longer excitation wavelength.[32, 33] As **DZ_{AS}-1~6** possess the typical D-π-A structure of two-photon probes, the two-photon absorption cross-sections (δ) of **DZ_{AS}** were determined by two-

10.1002/chem.201905183

photon induced fluorescence measurement technique (Fig. S13). As shown in Table S3 and Figure S22, **DZ_{AS}-1~6** display δ as high as 542 GM, and high photostability, implying that the **DZ_{AS}** could serve as two-photon fluorescent probes for bioimaging.

To evaluate their performance in cell imaging experiments, **DQ**, **DZ_A**, **DA_{AS}-1** and **DA_{AS}-2** were chosen as they display different colors. MTT assays were firstly performed and more than 85% of A549 cells survived after incubation with the probes (5.0 μM) for 24 h, indicating low cytotoxicity of the probes (Fig. S14~S17). The further time-dependent imaging experiments indicated that the cell could show the obviously signal after 30 min incubation (Figure S23). Subsequently, A549 cells were incubated with ethynylbenzene and treated with **DQ**, **DZ_A**, **DA_{AS}-1** and **DA_{AS}-2** and $CuSO_4·5H_2O$, sodium ascorbate, THPTA for 30 min. The turn-on fluorescence of various colors is clearly observed in living cells (Fig. S24). These results indicate that our newly developed light-up bio-orthogonal probes are suitable for living cell imaging study with multiple emission channels. In addition, **DA_A** was also demonstrated to be capable of imaging cell surface glycans successfully utilizing metabolic engineering approach (Fig. S25). These experiments showed that light-up bioorthogonal probes are capable of wash-free cell imaging study.

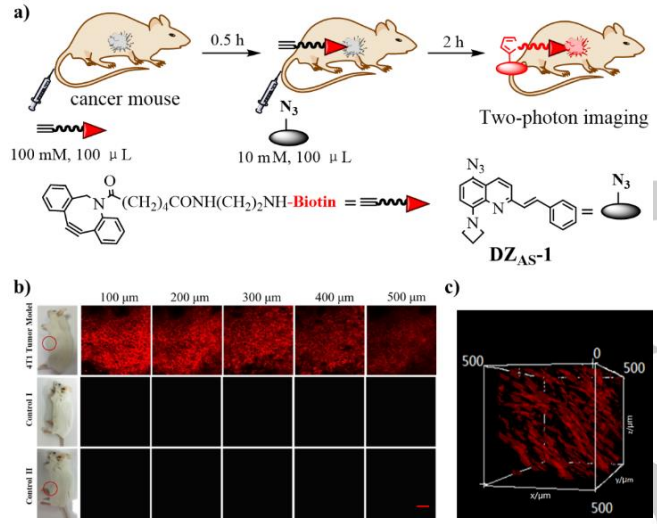

Fig. 5. In situ two-photon imaging of mice with tumor xenograft. a) Mice intravenous injected with DBCO-$(CH_2)_4CONH(CH_2)_2$NH-Biotin (100 mM, 100 μL)with subsequent intravenous injection (0.5 h later) of **DA_{AS}-1** (10 mM, 100 μL) in PBS. b) Two-photon imaging of mice with tumor xenograft after 2 h incubation. Control I: without tumor xenografts; control II: without addition of DBCO-conjugated biotin. c) 3D image of xenograft tumors in a living mouse. Images were acquired using 780 nm TP excitation with Olympus FVMPE-RS. TP fluorescence emission windows: 520−580 nm. Scale bar = 50 μm.

Next, we examined whether our probes can be used for two-photon in vivo imaging experiments. **DA_{AS}-1** was chosen in our study due to its good two-photon properties and relatively long-wavelength emission. *N, N*-dimethylprop-2-yn-1-amine and triphenyl phosphine-alkyne were used as targeting groups for lysosomes and mitochondria. Live A549 cells were firstly incubated with *N, N*-dimethylprop-2-yn-1-amine (mitochondrion-targeting group) and triphenyl phosphine-alkyne (lysosome-targeting group) respectively (Fig. S26-S27). Subsequently, **DA_{AS}-1** and click reaction cocktail were added, and after incubating at 37 ℃ for 2 h, and live cells were imaged by two-photon microscopy without washing steps. In addition, DND-99 and Mito-Red-FM were used as the tracker of lysosomes and mitochondria for comparison purpose. As shown in Fig. 4, cells treated with **DA_{AS}-1** after click reactions displayed enhanced fluorescent signals and the fluorescent images overlay well with the tracker dyes, whose overlap coefficient is 0.921 (for lysosome) and 0.902 (for mitochondria) respectively. These experiments demonstrated that these bioorthogonal light-up probes could distribute and turn on fluorescence in at specific location in living cells.

Encouraged by the above results, we further performed zebrafish imaging experiments using **DA_{AS}-1**. As shown in Fig. S28, using two-photon excitation microscopy, a substantial two-photon fluorescence signal could be detected in zebrafish treated with *N, N*-dimethylprop-2-yn-1-amine, $CuSO_4·5H_2O$, sodium ascorbate, THPTA and **DA_{AS}-1**. In contrast, no two-photon fluorescence signal was observed when the zebrafish was treated solely with **DA_{AS}-1**. These results indicated that the two-photon signal is attributed to the successful cycloaddition of the alkynyl group and **DA_{AS}-1**.

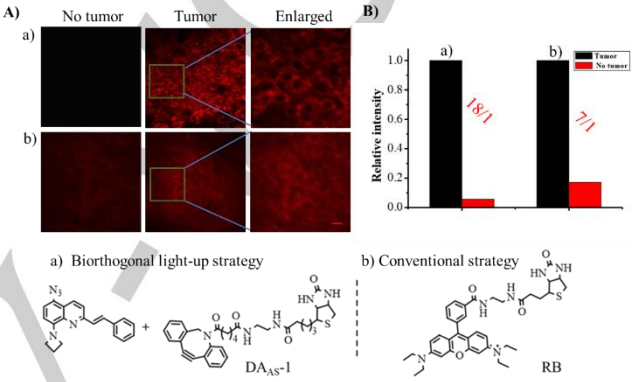

Fig. 6. In situ two-photon imaging of mice with tumor xenograft. A: a) bioorthogonal light-up imaging with **DA_{AS}-1** at a depth of 400 μm; b) conventional fluorescent imaging strategy with **RB** at a depth of 400 μm; B: Relative fluorescent intensity at a depth of 400 μm of tumor xenograft and no tumor xenograft. Mice was intravenously injected with DBCO-$(CH_2)_4CONH(CH_2)_2$NH-Biotin (100 mM, 100 μL) followed by subsequent intravenous injection (0.5 h later) of **DA_{AS}-1** (10 mM, 100 μL) in PBS.

In order to further expand the biological application scope of the probe, we performed in-vivo imaging experiments with **DA_{AS}-1** in mice. Biotin unit, as an effective tumor-targeting ligand for cancer imaging, has been successfully applied for tracking cancer cells and targeted drug delivery.[34-36] Consequently we selected the DBCO-$(CH_2)_4CONH(CH_2)_2$NH-Biotin as the tumor-targeting ligand for the subsequent biorthogonal imaging study of tumors (Fig. S30). To avoid the usage of catalyst copper ion which may be toxic to the mice, dibenzocyclooctyne was used for the copper-free click reaction.[37] Firstly, tumor xenografts were generated by standard protocol.[38, 39] Then, the tumor-bearing mice were intravenously injected with DBCO-$(CH_2)_4CONH(CH_2)_2$NH-Biotin (100 mM, 100 μL), followed by injection of the **DA_{AS}-1** (10 mM, 100 μL, Fig. 5) after 0.5 h. The same experiments were carried out with two additional control groups concurrently. The first control group was the mice without tumor xenografts, and the other control group utilized mouse tumor xenograft without treatment of DBCO-conjugated biotin (Control I and II, Fig. 5). After 2 h incubation, imaging of the tumor was carried out with two-photon excitation microscopy. As shown in Fig. 5b, a strong two-photon signal could be observed in the tumor tissue of the mice. In contrast, there were no signal observed in the control groups. Furthermore, the penetrating depth could reach deeper than 500 μm, which demonstrates that our probes are superior to all of the existing one-photon light-up probes (Figure S30- S31). In addition, 3D image of xenograft tumors in a living mouse was successfully constructed, which is difficult to acquire from one-photon microscopy. These results demonstrated that our probes

could be employed as a powerful and robust tool for two-photon in vivo imaging of tumors.[40]

To further explore advantages of our biorthogonal light-up probes, a conventional probe RB, in which biotin is connected directly with the rhodoamine B, was synthesized and employed for in vivo imaging. As shown in Fig. 6, in vivo fluorescence imaging of subcutaneous tumor demonstrated that conventional probe **RB** displayed stronger background with poor resolution (Fig. 6A), while the biorthogonal light-up probe (**DA_{AS}-1**) not only showed high resolution but also increase signal-to-noise ratio from 7 to 18 significantly (Fig. 6B). These results together strongly proved that our biorthogonal probes is more advantageous than the conventional probes.

Conclusions

A novel class of light-up bioorthogonal probes with color tunable from blue to orange was successfully developed. Generally, azido derivatives of AQ can produce large fluorescence after cycloaddition reaction. Remarkably, the replacement of amine with four-membered azetidine ring in AQ scaffold leads to significant fluorescence enhancement up to 1352-fold by effectively suppressing ICT effect. Interestingly, the substitution of styryl group at C-2 position exhibits long emission wavelength (up to 610 nm) and large two-photon absorption cross section (δ up to 542 GM). Subsequent bioimaging experiments demonstrate that these probes are versatile, which have been successfully used for live cell imaging without washing steps, and in-vivo two-photon imaging of live zebrafish and mice. Remarkably, these light-up biorthogonal probes with two-photon property displayed better resolution and higher signal to noise ratio for in vivo tumor imaging than conventional fluorophores without light-up property. It is also noteworthy that, the design strategy reported in this study represents a unique approach to realize a diversity of high-performance light-up biorthogonal probes for bioimaging. We envison that the bioorthognal probes developed in this study will provide useful tools for cancer diagnosis or fluorescence-guided therapy.

Experimental Section

Experimental Details see Supporting information

Acknowledgements

The authors are grateful to the National Natural Science Foundation of China (Nos. 21472172, 21272212, 51603186 & 21572190), Natural Science Foundation of Zhejiang Province (No. LY17B060009) and the City University of Hong Kong Grant (No. 9667147), the National University of Singapore (R279-000-482-133) and Singapore NRF (R279-000-444-281).

Keywords: Bioorthogonal reaction• fluorescence light-up • two-photon • 8-aminoquinoline • in vivo imaging

1. T. Yogo, K. Umezawa, M. Kamiya, R. Hino, Y. Urano, *Bioconjugate Chem.* **2017**, 28, 2069-2076.
2. Z. Li, D. Wang, L. Li, S. Pan, Z. Na, C. Y. J. Tan, S. Q. Yao, *J. Am. Chem. Soc.* **2014**, 136, 9990-9998.
3. B. Yuan, Y. Sun, Q. Guo, J. Huang, X. Yang, Y. Y. Chen, X. H. Wen, Xi. Meng, J. Liu, K. Wang, *Anal. Chem*. **2017**, 89, 9347-9353.
4. H. X. Wu, J. Yang, J. Seckute, N. K. Devaraj, *Angew. Chem. Int. Ed.* **2014**, 53, 5805-5809.
5. P. Agarwal, B. J. Beahm, P. Shieh, C. R. Bertozzi, *Angew. Chem. Int. Ed*. **2015**, 54, 11504-11510.
6. Y. C. Chen, C. M. Clouthier, K. Tsao, M. Strmiskova, H. Lachance, J. W. Keillor, *Angew. Chem. Int. Ed*. **2014**, 53, 13785-13788.
7. Q. Li, T. Dong, X. H. Liu, X. Lei, *J. Am. Chem. Soc.* **2013**, 135, 4996−4999.
8. L. Xu, R. C. Cooper, J. Wang, W. A. Yeudall, H. Yang. *ACS Biomater. Sci. Eng.* **2017**, 3, 1641−1653.
9. Devaraj N. K. *ACS Cent. Sci.* **2018**, 4, 952−959.
10. A. E. Speers, G. C. Adam, B. F. Cravatt, *J. Am. Chem. Soc.* **2003**, 125, 4686-4687.
11. L. I. Willems, H. S. Overkleeft, S. I. Kasteren, Bioconjugate Chem., 2014, 25, 1181-1191
12. S. Zhuang, Q. Li, L. Cai, C. Wang, X. Lei, *ACS Cent. Sci*. **2017**, 3, 501-509.
13. M. Li, X. Zhou, S. Guo, N. Wu, *Biosens. Bioelectron.* **2013**, 43, 69-74.
14. X. L. Zhang, C. Zheng, S. S. Guo, J. Li, H. H. Yang, G. Chen, *Anal. Chem.* **2014**, 86, 3426-3434.
15. S. Reymond, J. Cossy, *Chem. Rev*. **2008**, 108, 5359–5406.
16. X. X. Jiang, R. Wang, *Chem. Rev.* **2013**, 113, 5515−5546.
17. X. Shang, X. Song, C. Faller, R. Lai, H. Li, R. Cerny, W. Niu, J. Guo, *Chem. Sci*., **2017**, 8, 1141-1145.
18. J. J. Shie, Y. C. Liu, Y. M. Lee, C. Lim, J. M. Fang, C. H. Wong, *Chem. Commun.* **2017**, 53, 1490-1493.
19. P. Shieh, V. T. Dien, B. J. Beahm, J. M. Castellano, T. W. Coray, C. R. Bertozzi, *Chem. Sci.* **2015**, 137, 7145−7151.
20. Y. J. Lee, W. Cho, J. Sung, E. Kim, S. B. Park, *J. Am. Chem. Soc.* **2018**, 140, 974-983.
21. F. B. Yu, P. Li, P. Song, B. S. Wang, J. Z. Zhao, K. Han, *Chem. Commun.* **2012**, 48, 2852-2854.
22. Q. Y. Xu, L. W. He, H. P. Wei, W. Y. Lin, *J. Fluoresc.* **2018**, 28, 5-11.
23. R. J. Mellanby, J. I. Scott, I. Mair, A. Fernandez, L. Saul, J. Arlt, M. Moral, M. Vendrell, *Chem. Sci.* **2018**, 9, 7261-7270.
24. Y. Dou, Z. Xie, Z. Sun, H. Fang, C. Shen, P. Zhang, Q. Zhu, *ChemCatChem,* **2016**, 8, 3570-3574.
25. Y. Dou, X. Gu, S. Ying, S. Zhu, S. A. Yu, W. Shen, Q. Zhu, *Org. Biomol. Chem.* **2018**, 16, 712–716.
26. K. M. Zhang, W. Dou, X. L. Tang, L. Z. Yang, Z. H. Ju, Y. M. Cui, W. S. Liu, *Tetrahedron Lett*. **2015**, 56, 2707–2709.
27. Z. Gao, X. Zhang, M. Zhang, Y. Chen, *Dyes Pig.* **2013**, 99, 531-536.
28. Z. Y. Hao, S. L. Hong, X. Chen, P. R. Chen, *Acc. Chem. Res*. **2011**, 44, 742-751.
29. K. Lang, J. W. Chin, *ACS Chem. Biol.* **2014**, 9, 16-20.
30. A. Kumar, M. D. Sevilla, *J. Phys. Chem. A.* **2019**, 123, 3098-3108.
31. a) J. S. Seixas, R. S. Becker, A. L. Macanita, *J. Phys. Chem.* **1994**, 98, 6054-6058; b) Zhou Z., Fahrni C. J., *J. Am. Chem. Soc.* **2004**, 126, 8862-8863; c) J. A. Gonzalez-Vera, E. Lukovic, B. Imperiali, *J. Org. Chem.* **2009**, 74, 7309–7314, d) M. Ghedini, M. L. Deda, L. Aiello, A. Grisolia, *Inorg. Chim. Acta*, **2004**, 357, 33–40.
32. F. Helmchen, W. Denk, *Nat Methods*. **2005**, 2, 932-940.
33. Y. H. Li, Y. Sun, J. C. Li, Q. Q. Su, W. Yuan, Y. Dai, C. M. Han, Q. H. Wang, W. Feng, F. Y. Li, *J. Am. Chem. Soc*. **2015**, 137, 6407−6416.
34. D. Jung, S. Maiti, J. H. Lee, J. H. Lee, J. S. Kim, *Chem. Commun.* **2014**, 50, 3044-3048.
35. X. Q. Kong, B. L. Dong, N. Zhang, C. Wang, X. Z. Song, W. Y. Lin, *Talanta,* **2017**, 174, 357–364.
36. H. M. Kim, B. R. Cho, *Chem. Rev*. **2015**, 115, 5014−5055.

10.1002/chem.201905183

37. S. V. Orski, A. A. Poloukhtine, S. Arumugam, L. Mao, V. V. Popik, J. Locklin, *J. Am. Chem. Soc.* **2010**, 132, 11024–11026.
38. W. Zhang, P. Li, F. Yang, X. F. Hu, C. Z. Sun, W. Zhang, D. Z. Chen, B. Tang, *J. Am. Chem. Soc*. **2013**, 135, 14956−14959.
39. C Y. Dong S. J. Yang, J. Y. Shi, H. Y. Zhao, L. J. Zhong, Z. F. Liu, B.Jia, F. Wang, *Sci Rep.* **2015**, 6, 18905.
40. Y. Liang, J. L. Mackey, S. A. Lopez, Fang Liu, K. N. Houk, *J. Am. Chem. Soc.* **2012**, 134, 17904-17907.

10.1002/chem.201905183

WILEY-VCH

Layout 2:

FULL PAPER

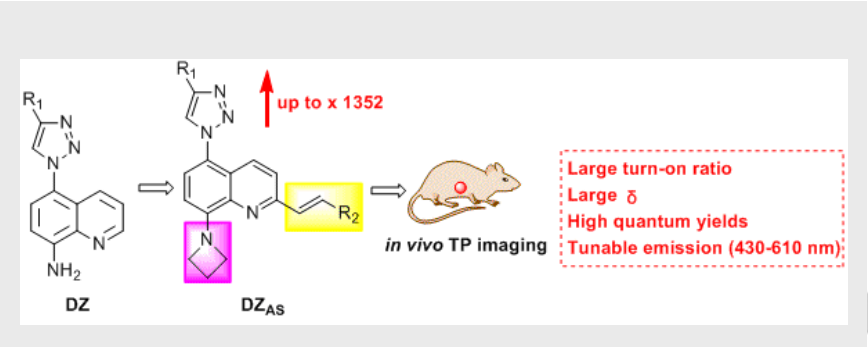

Yandong Dou, [+][a] Yajun Wang, [+][a] Yukun Duan,[b] Bin Liu,[*][b] Qinglian Hu,[a] Wei Shen,[*][c] Hongyan Sun[*][d] and Qing Zhu[*][a]

Page No. – Page No.

Color-Tunable Light-up Bioorthogonal Probes for *in-vivo* Two-Photon Fluorescence Imaging